

Compressive beamforming and directional sound reconstruction using the Kronecker array transform

Marcelo A. Daher, Carlos A. Prete Jr., Vítor H. Nascimento
Dept. of Electronic Systems Engineering
University of São Paulo
São Paulo, Brazil
{marcelo.daher,carlos.prete,vitnasci}@usp.br

Bruno S. Masiero
Dept. of Communications
University of Campinas
Campinas, Brazil
masiero@unicamp.br

Abstract—The Kronecker array transform (KAT) was introduced to reduce the computational burden in acoustic image estimation and other 2-dimensional array processing applications. The KAT can be applied only when the planar microphone array is *separable*. In this paper we study the performance of separable arrays using compressive beamforming algorithms to estimate the direction of arrival (DOA) of far-field sources and to recover the signal arriving from a particular direction. Our analysis extends previous studies based on mutual coherence to separable arrays, and shows that non-redundant separable arrays have better mutual coherence than can be obtained using 2D random arrays. We also derive the space discretization that yields the minimum coherence, and study the influence of frequency and the spatial resolution on the coherence. In order to verify the results, we present the performance of a separable array in two problems: DOA estimation and signal recovery using sparse reconstruction, and compare its performance with classical beamforming techniques. The sparsity-based approach shows better performance in DOA estimation and great improvement in time-domain signal recovery.

Index Terms—Microphone arrays, beamforming, source separation, signal denoising, compressed sensing.

I. INTRODUCTION

The Kronecker array transform (KAT) was introduced with the goal of reducing computations in algorithms for acoustic image estimation under the condition that the microphone array is designed with a *separable* geometry [1], [2]. The KAT can be applied to a number of different acoustic imaging algorithms [2], such as conventional beamforming [3], DAMAS [4], and covariance-fitting [5]. Moreover, the KAT has been recently extended to more general beamforming applications in [6]. And although the use of regularized optimization [5] and sparse estimation techniques [2] has been proposed in order to achieve better resolution of the acoustic images, using either ℓ_1 or total variation regularization, the performance of the accelerated algorithms was not studied from a compressive sensing point of view.

Application of compressive sensing ideas to beamforming has been proposed in [7], [8] and, more recently, Xenaki et al. [9] studied the performance of direction-of-arrival (DOA) algorithms based on compressive sensing, considering one-dimensional random arrays, relating performance measures (such as resolution) to the coherence of the measurement matrix. The performance of nonrandom arrays was considered

in [10], which used an extension of the restricted isometry condition (RIP) to find the probability that a set of k -sparse source directions will be recovered.

In this paper we study the performance of separable arrays in recovering the directions, intensities and the actual time-signals of a small number of sound sources impinging on a two-dimensional array. Our analysis is based on the coherence of the measurement matrix (following [9]), but extending previous results in four ways: (i) we consider two-dimensional arrays, (ii) we consider separable arrays for which the KAT can be applied, (iii) we evaluate the performance as a function of the signal frequency, and (iv) we evaluate the recovery of the time signals. A further contribution is our analysis of the best way to discretize the look directions. Although there are methods to improve the resolution of compressive-sensing beamforming techniques, using grid refinement or the atomic norm [11], our analysis is restricted in this paper to a fixed, finite number of look directions. In addition, although there are source localization methods for broadband signals that consider the full spectrum of the signal [12], we show here that, in the case of a small number of sources, processing each frequency independently already gives good results for the reconstruction of the time signal coming from a particular direction.

The remainder of this paper is organized as follows. In Section II we describe the signal model, while Section III describes the assumptions on the array and look directions for application of the Kronecker array transform. Section IV compares the coherence of measurement matrices obtained from different choices of arrays as a function of the signal frequency, and Section V finds the space discretization that results in minimal coherence. Section VI shows the performance of the chosen separable array with DOA estimation, Section VII considers the problem of signal recovery, and Section VIII concludes the paper.

II. PROBLEM OVERVIEW

Consider a microphone array with N_{Mic} microphones, receiving signals from sources in the far field, discretized in N_{Dir} directions of interest. Each direction is represented by a unitary vector \mathbf{u} , perpendicular to the plane wave traveling from this

direction. The vector \mathbf{u} is defined in spherical coordinates in terms of the polar angle θ and the azimuthal angle ϕ as

$$\mathbf{u} = \begin{bmatrix} u_x \\ u_y \\ \sqrt{1 - u_x^2 - u_y^2} \end{bmatrix} = \begin{bmatrix} \sin \theta \cos \phi \\ \sin \theta \sin \phi \\ \cos \theta \end{bmatrix}. \quad (1)$$

Given a signal coming from the direction \mathbf{u} and the position \mathbf{p}_i of the i -th microphone, we can calculate the time delay τ_i , with respect to the origin, for the signal to reach each microphone, as $\tau_i = -\frac{\mathbf{u}^T \mathbf{p}_i}{c}$, where c is the speed of sound in the medium.

For a given direction \mathbf{u} and an angular frequency ω , we define a delay vector $\mathbf{v}(\omega : \mathbf{u})$ containing the frequency delays of a given direction for the N_{Mic} microphones in our array

$$\mathbf{v}(\omega : \mathbf{u}) = \begin{bmatrix} e^{j\omega\tau_0} \\ e^{j\omega\tau_1} \\ \vdots \\ e^{j\omega\tau_{(N_{\text{Mic}}-1)}} \end{bmatrix} = \begin{bmatrix} e^{-j\omega\mathbf{u}^T \mathbf{p}_0/c} \\ e^{-j\omega\mathbf{u}^T \mathbf{p}_1/c} \\ \vdots \\ e^{-j\omega\mathbf{u}^T \mathbf{p}_{(N_{\text{Mic}}-1)}/c} \end{bmatrix}. \quad (2)$$

Once the N_{Dir} directions we will look at are chosen, we define an $[N_{\text{Mic}} \times N_{\text{Dir}}]$ matrix

$$\mathbf{V}(\omega) = [\mathbf{v}(\omega : \mathbf{u}_0); \mathbf{v}(\omega : \mathbf{u}_1); \cdots; \mathbf{v}(\omega : \mathbf{u}_{(N_{\text{Dir}}-1)})]. \quad (3)$$

We also define the vector $\mathbf{x}(\omega)$ containing the windowed Discrete Fourier Transforms of the signal from all microphones for a frequency $\omega = k2\pi/L$, $0 \leq k \leq L-1$, where L is the DFT length, and the vector $\mathbf{y}(\omega)$ containing the far field signals arriving from each direction:

$$\mathbf{x}(\omega) = [x_0(\omega), x_1(\omega), \cdots, x_{N_{\text{Mic}}-1}(\omega)]^T, \quad (4)$$

$$\mathbf{y}(\omega) = [y_0(\omega), y_1(\omega), \cdots, y_{N_{\text{Dir}}-1}(\omega)]^T. \quad (5)$$

In our model, the signal vector $\mathbf{x}(\omega)$ received by the microphone array is the sum of the $\mathbf{y}(\omega)$ signals with the correspondent delays applied for each microphone, thus

$$\mathbf{x}(\omega) = \mathbf{V}(\omega) \cdot \mathbf{y}(\omega). \quad (6)$$

Our goal is to recover $\mathbf{y}(\omega)$ from $\mathbf{x}(\omega)$ and $\mathbf{V}(\omega)$, which is an ill-posed problem. We compare the quality of the estimates $\hat{\mathbf{y}}(\omega)$ obtained for all frequencies of interest by sparse methods with the Delay-and-Sum (DAS) beamformer and the Minimum Variance Distortionless Response (MVDR) beamformer [13], as well as the reconstructions of the time signals $y_k(t)$, $k = 0, \dots, N_{\text{dir}} - 1$.

III. SEPARABLE ARRAYS

When working with a 2-dimensional microphone array, we can design our system in a specific way to allow the decomposition of the matrix \mathbf{V} as a Kronecker product of two other matrices, enabling us to explore properties of the Kronecker product to accelerate our computations [2], [6]. This is done by choosing the microphone positions in our array and the directions of interest in a separable format.

A 2D separable array has $N_{\text{Mic}} = N_{\text{MicX}} \times N_{\text{MicY}}$ microphones on the positions $(x, y) = (x_i, y_j)$, where $i =$

$1, \dots, N_{\text{MicX}}$ and $j = 1, \dots, N_{\text{MicY}}$. Following the same idea, a 2D separable grid maps $N_{\text{DirX}} \times N_{\text{DirY}} = N_{\text{Dir}}$ \mathbf{u} directions, defined by the first two entries of (1), $(u_x, u_y) = (u_{xi}, u_{yj})$, where $i = 1, \dots, N_{\text{DirX}}$ and $j = 1, \dots, N_{\text{DirY}}$.

If both the array and the discrete acoustic grid are separable, our sensing matrix \mathbf{V} can be decomposed as the Kronecker product of two other matrices [1], [6]:

$$\mathbf{V} = \mathbf{V}_x \otimes \mathbf{V}_y. \quad (7)$$

The use of separable arrays allows us to use properties of the Kronecker Product to reduce the computational complexity of beamforming and sparse reconstruction algorithms, as shown in [2], [14], with gains of up to $\sqrt{\min\{N_{\text{Dir}}, N_{\text{Mic}}\}}$ operations.

For the simulations in this article, a deterministic array geometry is used instead of a random geometry as suggested in [9]. A 30 cm linear non-redundant spacings (minimum missing lags) array [15] is extended to two dimensions as described in [16], [17]. Although we are using an extended 8-microphone non-redundant array, any other linear array geometry, such as uniform linear arrays or a co-prime array [18], can be extended to a 2D separable array configuration.

We define the directions \mathbf{u} on the discrete grid by uniformly spacing u_x and u_y between $[-1, 1]$, creating a $[33 \times 33]$ separable grid. As a consequence, some \mathbf{u} vectors represent invalid directions, such as $\mathbf{u} = [1, 1, \sqrt{-1}]^T$, thus estimates from these spurious directions are ignored. The vector of directions of interest \mathbf{u} is uniformly spaced because this distribution yields the minimum coherence for low frequencies and separable arrays, as shown in Section V.

IV. SPARSE RECONSTRUCTION

We use sparse reconstruction techniques to recover an estimate $\hat{\mathbf{y}}(\omega)$ from equation (6) given the manifold matrix \mathbf{V} (obtained from our system's design) and the measurement vector \mathbf{x} .

To assess our array geometry, we look at the coherence of $\mathbf{V}(\omega)$ as a function of the frequency we are reconstructing. The coherence of a matrix \mathbf{A} with normalized columns is an intuitive measure of the correlation between its columns, defined as [19]

$$\mu(\mathbf{A}) = \max_{i \neq j} \mathbf{G}_{ij}, \quad \mathbf{G} = |\mathbf{A}^H \mathbf{A}|, \quad (8)$$

where \mathbf{G}_{ij} is the element on the i th row and j th column of the Gram matrix \mathbf{G} . Note that the columns of $\frac{1}{\sqrt{N_{\text{Mic}}}} \mathbf{V}$ are normalized.

The coherence of a matrix can give us guarantees that our solution is optimally sparse and unique if certain conditions are satisfied. If equation $\mathbf{A}\mathbf{x} = \mathbf{b}$ has a solution vector \mathbf{x} such that

$$\|\mathbf{x}\|_0 < \frac{1}{2} (1 + \mu(\mathbf{A})^{-1}), \quad (9)$$

then \mathbf{x} is the unique solution with the minimum number of nonzero elements (ℓ_0 norm) [19]–[21]. Therefore, the lower the coherence, the larger the number of nonzero elements that can be uniquely recovered. On the other hand, if the signal is corrupted by noise (thus $\mathbf{A}\mathbf{x} \approx \mathbf{b}$), some sparse estimation

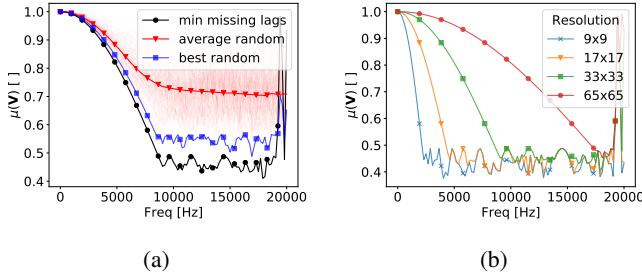


Figure 1: $\mu(\mathbf{V})$ vs frequency for 30 cm 8×8 microphones minimum missing lags (a) vs. random arrays of similar dimension, and (b) increasing for low frequencies as the resolution increases

algorithms provide theoretical bounds for the reconstruction error that are tighter for lower coherence [22], [23].

For separable arrays, the property [24]

$$\mu(\mathbf{V}) = \mu(\mathbf{V}_x \otimes \mathbf{V}_y) = \max(\mu(\mathbf{V}_x), \mu(\mathbf{V}_y)) \quad (10)$$

can be used to analyze the coherence of the sensing matrix. This allows us to extrapolate the analysis from [9] to a 2-dimensional system, setting $\mu(\mathbf{V})$ as a parameter for the array performance when using compressive sensing for signal reconstruction or DOA estimation.

Given our chosen array reconstructing a $[33 \times 33]$ discrete uniform field, both described in Section III, the coherence of our sensing matrix as a function of the frequency is seen on Fig. 1a, along with that of several random arrays of similar dimensions. We can see that the non-redundant array has the smallest coherence for almost all the frequency range. From the illustrated data, we can expect this array geometry to perform best when reconstructing signals with main components between 9 kHz and 18 kHz.

As we increase the resolution of the reconstructed image, the lower frequency limit of the region of small coherence increases (see eq. (15) in section V), reducing the region with small coherence. This effect is illustrated in Fig. 1b and can be explained in the following manner: as we increase resolution the look directions get closer together, turning the neighboring columns of \mathbf{V} more similar and, therefore, increasing its coherence.

V. MINIMAL COHERENCE SPACE DISCRETIZATION

In this section, we prove that a uniformly distributed scan grid yields the minimum coherence for low frequencies and separable array geometry. First, we show this statement for 1D arrays, where $\mathbf{p} = [p \ 0 \ 0]^T$ and $\mathbf{u} = [u \ 0 \ \sqrt{1-u^2}]^T$, and then we generalize this result for 2D separable arrays.

Considering the 1D case, define the function $g_{m,n}(\omega)$ as

$$g_{m,n}(\omega) = \frac{1}{N_{\text{Mic}}^2} |\mathbf{v}(\omega : \mathbf{u}_m)^H \mathbf{v}(\omega : \mathbf{u}_n)|^2, \quad m \neq n \quad (11)$$

and set $g_{m,n} = 0$ if $m = n$. This way, the coherence is $\mu(\mathbf{V}) = \max_{m,n} \sqrt{g_{m,n}(\omega)}$. Substituting $[\mathbf{v}(\omega : \mathbf{u}_i)]_k = e^{-j\frac{\omega}{c} u_i p_k}$ in (11), we have

$$g_{m,n}(\omega) = \frac{1}{N_{\text{Mic}}^2} \sum_{k=0}^{N_{\text{Mic}}-1} \sum_{\ell=0}^{N_{\text{Mic}}-1} e^{-j\frac{\omega}{c} (u_m - u_n)(p_k - p_\ell)}. \quad (12)$$

Note that $g_{m,n}(0) = 1$ for all m, n , therefore the worst-case coherence will occur for low frequencies. For each term $e^{-j\frac{\omega}{c} (u_m - u_n)(p_k - p_\ell)}$ in the sum with $k \neq \ell$, there is a single term $e^{-j\frac{\omega}{c} (u_m - u_n)(p_\ell - p_k)}$, which is the conjugate of the first term. Since the sum of these two terms is $2 \cos(\frac{\omega}{c} (u_m - u_n)(p_k - p_\ell))$ and the sum of the terms with $k = \ell$ is $\frac{1}{N_{\text{Mic}}}$, (12) can be rewritten as

$$g_{m,n}(\omega) = \frac{1}{N_{\text{Mic}}} + \frac{2}{N_{\text{Mic}}^2} \sum_{k=0}^{N_{\text{Mic}}-1} \sum_{\ell=k+1}^{N_{\text{Mic}}-1} \cos\left(\frac{\omega}{c} (u_m - u_n)(p_k - p_\ell)\right). \quad (13)$$

Consider that ω is small enough such that

$$\mu(\mathbf{V})^2 = g_{m^*, n^*}(\omega), \quad (m^*, n^*) = \arg \min_{m,n} |u_m - u_n|. \quad (14)$$

Equation (14) is true if ω is very small so that each cosine being summed in (13) is a decreasing function with respect to $|u_m - u_n|$, as in this case $g_{m,n}(\omega)$ would be maximized by picking m and n such that $|u_m - u_n|$ is minimum. Since $\mu(\mathbf{V})$ is a continuous function of ω , (14) remains true until ω is high enough so that $g_{m,n}(\omega) = g_{m^*, n^*}(\omega)$ for some $m \neq m^*$ and $n \neq n^*$. This way, $\mu(\mathbf{V})^2 = g_{m^*, n^*}(\omega)$ if $0 < \omega \leq \omega^*$, where

$$\omega^* = \min_{\omega > 0} \{\omega : \mu(\mathbf{V}) = g_{m^*, n^*}(\omega)\}. \quad (15)$$

Our objective is to obtain the best $(u_0, u_1, \dots, u_{N_{\text{Dir}}-1})$ such that the coherence $\mu(\mathbf{V})$ is minimum, which is achieved by minimizing $\mu(\mathbf{V})^2$. Defining $\omega_1 > 0$ as the smallest critical point of $g_{m^*, n^*}(\omega)$, $\mu(\mathbf{V})^2$ is a decreasing function with respect to Δu^* for $\omega < \min\{\omega^*, \omega_1\}$, so Δu^* must be maximized. In other words, the set $\{u_i\}_{i=0}^{N_{\text{Dir}}-1}$ that yields the lowest coherence can be obtained by solving the following constrained optimization problem:

$$(u_0^*, \dots, u_{N_{\text{Dir}}-1}^*) = \arg \max_{u_0, \dots, u_{N_{\text{Dir}}-1}} \min_i \{u_i - u_{i-1}\} \\ \text{s.t. } -1 \leq u_0 \leq u_1 \leq \dots \leq u_{N_{\text{Dir}}-1} \leq 1 \quad (16)$$

Although this may seem a difficult problem, its solution is straightforward: (16) must satisfy $u_i^* - u_{i-1}^* = \text{constant} \forall i$ because if it were not constant, $u_k^* - u_{k-1}^* = \min_i u_i^* - u_{i-1}^*$ could be increased by slightly increasing the value of $u_k^* - u_{k-1}^*$ such that k remains the index that minimizes $u_i^* - u_{i-1}^*$, thus $u_k^* - u_{k-1}^*$ would not maximize the expression. Furthermore, in order to maximize the minimum interval between u_i and u_{i-1} , the distance between the highest and the lowest element of $\{u_i\}_{i=0}^{N_{\text{Dir}}-1}$ must be as high as possible. As each u_i lies in the interval $[-1, 1]$, we must have $u_0^* = -1$ and $u_{N_{\text{Dir}}-1}^* = 1$.

Consequently, the solution for (16) is linearly spaced between -1 and $+1$:

$$u_i^* = -1 + \frac{2}{N_{\text{Dir}} - 1}k, \quad 0 \leq k \leq N_{\text{Dir}} - 1. \quad (17)$$

Therefore, the minimal coherence space discretization is the uniform distribution if $0 < \omega < \min\{\omega^*, \omega_1\}$, where ω^* is given by (15) and ω_1 is the smallest frequency such that $\frac{d}{d\omega}g_{m^*,n^*}(\omega) = 0$. Even though ω^* has no closed-form expression, it can be calculated numerically using (15). For instance, using our non-redundant array with $N_{\text{Mic}} = 8$, $N_{\text{Dir}} = 33$ and $c = 343$ m/s, we have $\omega_1 = 2\pi \times 12.64$ krad/s and $\omega^* = 2\pi \times 9.17$ krad/s, which agrees with Fig. 1a.

For two-dimensional separable arrays, $\mathbf{u} = [u_x \ u_y \ \sqrt{1-u_x^2-u_y^2}]^T$ and $\mu(\mathbf{V}) = \max\{\mu(\mathbf{V}_x), \mu(\mathbf{V}_y)\}$. The minimal value for $\mu(\mathbf{V})$ can only be achieved when both $\mu(\mathbf{V}_x)$ and $\mu(\mathbf{V}_y)$ are minimized, which happens when both u_x and u_y follow the uniform distribution (17).

VI. DOA ESTIMATION

In this section, we verify our results using a separable array to estimate the direction of arrival (DOA) of a sinusoidal source at a random location with a sinusoidal interference fixed at the central position $(0, 0)$, and measurement noise with SNR of 30dB, with sampling frequency of 64kHz and FFTs with $L = 100$ points using a rectangular window with 100 points. The DOA of the source of interest is obtained using a single snapshot by Delay-and-Sum (DAS) beamformers and by sparse estimation using Orthogonal Matching Pursuit (OMP) [25], [26]. We also include results obtained using Regularized Minimum Variance Distortionless Response (Regularized MVDR) beamformers, designed with the exact noise covariance matrix (used as a benchmark). In practice MVDR beamformers need to estimate the noise covariance matrix, so they are not applicable to the single snapshot case. Since MUSIC [27] also needs multiple snapshots, we do not include it in our simulations. The simulations assume both the source and the interference to be sinusoids with the same magnitude and frequency f_0 and random phase. All three algorithms search a grid with 33×33 equally-spaced directions. To determine the precision of a single reconstruction, we assume previous knowledge of the number of sources present. The two largest values on the reconstructed image are considered the located sources, and the angle between the source of interest and the nearest of the two located sources is taken as the location error.

The DAS beamformer requires no configuration parameters, and its implementation uses the separability of the matrix \mathbf{V} through the Kronecker Product (eq. (7)) to reduce its computational complexity. The regularized MVDR is a variation on the MVDR beamformer initially proposed in [13], with an added constant in the main diagonal of the noise covariance matrix to provide robustness (diagonal loading) [28]. The diagonal regularization added is of value 10^{-2} . MVDR beamforming requires previous knowledge of the noise covariance matrix, and in this article the OMP algorithm is not fed this information. The OMP algorithm was set for 1% maximum sparsity

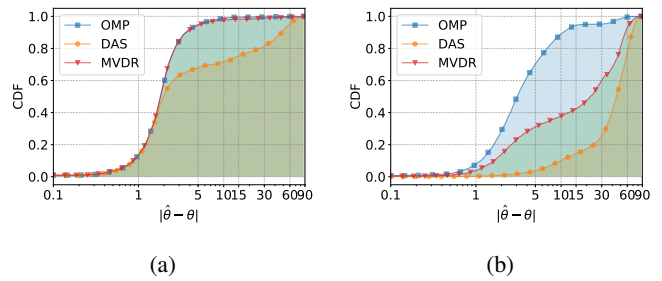


Figure 2: DOA error cumulative distribution for different algorithms at (a) 16 kHz and (b) 2 kHz

and 10^{-3} error stop condition. It also uses the separability of the matrix \mathbf{V} through the Kronecker product to accelerate its computations, as described in [6], [14].

After 6×10^3 realizations of the DOA experiment with random directions, we calculate the DOA error distribution for each algorithm. Fig. 2a represents the cumulative distribution function of the angular error $|\hat{\theta} - \theta|$ for $f_0 = 16$ kHz, a frequency in the low coherence region for the array, and Fig. 2b is for $f_0 = 2$ kHz, a frequency with a higher coherence (see Fig. 1a). From these results, we expect smaller deviations from the ideal DOA when using the OMP, even in low frequencies with high coherence.

It is worth noting that, in the exceptional case where all signal directions are in the reconstruction grid, since MVDR has full noise covariance information, it presents zero DOA error for all in-grid directions.

VII. SIGNAL RECOVERY

Our goal with this simulation is to recover an arbitrary signal coming from a specific direction, while there is a second signal source in the field that will be treated as noise. The signal estimation is obtained by recovering $\mathbf{x}(\omega)$ estimates for all ω in our Discrete Fourier Transform, and performing the inverse transform to obtain the signal in the time domain.

For the signal recovery, STFT is used with the Hanning window with 50% overlap as recommended in [29], [30]. We also pad our signal with zeros at the end of the window, doubling its size, as [31] suggests to mitigate time aliasing effects. We compare the reconstruction results obtained by using the compressive sensing algorithm OMP with those obtained with DAS and regularized MVDR beamformers. The parameter settings for the algorithms are the same as discussed on section VI.

The simulations were run reconstructing a $[33 \times 33]$ field, with the desired signal coming from the central direction $\mathbf{u}_s = [0 \ 0 \ 1]^T$, first with the signal being a filtered white noise with 11 kHz – 17 kHz bandwidth, to operate within the best coherence margin of the array, as seen on Fig. 1a, and a second case where the signal bandwidth is 2 kHz – 17 kHz, outside the low coherence region. The interference signal comes from the direction $\mathbf{u}_n = [0 \ \frac{-1}{2} \ \frac{\sqrt{3}}{2}]^T$, its signal being a filtered white noise with 0 – 18 kHz bandwidth. Independent Gaussian noise is added to each microphone to create measurement noise with

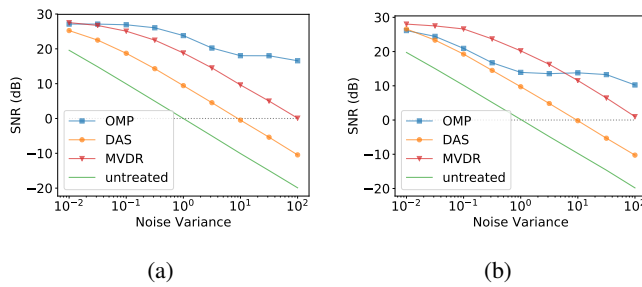


Figure 3: Reconstruction SNR vs interference variance for (a) 11 kHz - 17 kHz signal and (b) 2 kHz - 17 kHz

30 dB Signal-to-Noise Ratio and 150 realizations of each case were performed.

The SNR for the recovered signals are illustrated in Fig. 3, where *untreated* represents the SNR for the direct signal captured by a microphone located at position $[0, 0]$.

VIII. CONCLUSION

Compressive sensing was shown in [9] to be an effective solution for the one-dimensional source localization problem when working with sensor arrays. We extended this result to 2D source localization. We also show that compressive sensing techniques can be used to reconstruct the signal coming from a specific direction, similar to a super-directional microphone.

For both applications we show that more precise results than traditional beamformers can be expected from the OMP method, without the prior knowledge that MVDR requires. There are still topics to be explored further, such as carrying over information between frequency bins when working with wideband reconstruction, as [12], and using DOA knowledge as a starting point for the support in the sparse reconstruction.

REFERENCES

- [1] F. P. Ribeiro and V. H. Nascimento, "Fast transforms for acoustic imaging— part I: Theory," *IEEE Transactions on Image Processing*, vol. 20, no. 8, pp. 2229–2240, 2011.
- [2] —, "Fast transforms for acoustic imaging—part II: Applications," *IEEE Transactions on Image Processing*, vol. 20, no. 8, pp. 2241–2247, 2011.
- [3] H. L. Van Trees, *Optimum Array Processing: Part IV of Detection, Estimation, and Modulation Theory*. New York, NY: John Wiley & Sons, 2002.
- [4] T. F. Brooks and W. M. Humphreys, "A deconvolution approach for the mapping of acoustic sources (DAMAS) determined from phased microphone arrays," *Journal of Sound and Vibration*, vol. 294, no. 4, pp. 856–879, 2006.
- [5] T. Yardibi, J. Li, P. Stoica, N. S. Zawodny, and L. N. C. Iii, "A covariance fitting approach for correlated acoustic source mapping," *The Journal of the Acoustical Society of America*, vol. 127, no. 5, pp. 2920–2931, May 2010, 00014.
- [6] B. Masiero and V. H. Nascimento, "Revisiting the Kronecker array transform," *IEEE Signal Processing Letters*, vol. 24, no. 5, pp. 525–529, May 2017.
- [7] A. C. Gurbuz, J. H. McClellan, and V. Cevher, "A compressive beamforming method," in *Proc. Speech and Signal Processing 2008 IEEE Int. Conf. Acoustics*, Mar. 2008, pp. 2617–2620.
- [8] G. F. Edelmann and C. F. Gaumond, "Beamforming using compressive sensing," *The Journal of the Acoustical Society of America*, vol. 130, no. 4, pp. EL232–EL237, 2011.

- [9] A. Xenaki, P. Gerstoft, and K. Mosegaard, "Compressive beamforming," *The Journal of the Acoustical Society of America*, vol. 136, p. 260, 07 2014.
- [10] C. F. Gaumond and G. F. Edelmann, "Sparse array design using statistical restricted isometry property," *The Journal of the Acoustical Society of America*, vol. 134, no. 2, pp. EL191–EL197, 2013.
- [11] A. Xenaki and P. Gerstoft, "Grid-free compressive beamforming," *The Journal of the Acoustical Society of America*, vol. 137, no. 4, pp. 1923–1935, 2015.
- [12] L. Xu, K. Zhao, J. Li, and P. Stoica, "Wideband source localization using sparse learning via iterative minimization," *Signal Processing*, vol. 93, no. 12, pp. 3504–3514, 2013.
- [13] J. Capon, "High-resolution frequency-wavenumber spectrum analysis," *Proceedings of the IEEE*, vol. 57, no. 8, pp. 1408–1418, Aug 1969.
- [14] V. H. Nascimento, M. C. Silva, and B. S. Masiero, "Acoustic image estimation using fast transforms," in *Sensor Array and Multichannel Signal Processing Workshop (SAM), 2016 IEEE*. IEEE, 2016, pp. 1–5.
- [15] E. Vertatschitsch and S. Haykin, "Nonredundant arrays," *Proceedings of the IEEE*, vol. 74, no. 1, pp. 217–217, Jan 1986.
- [16] F. P. RIBEIRO, "Arrays de microfones para medida de campos acusticos," Ph.D. dissertation, Escola Politecnica, Universidade de Sao Paulo, 2012.
- [17] B. S. Masiero, C. S. B. Arroyo, and V. H. Nascimento, "Fast acoustic imaging with separable arrays," in *Proceedings, 2015 International Symposium on Solid Mechanics*, Belo Horizonte, MG, Brazil, May 2015, pp. 1–15.
- [18] P. P. Vaidyanathan and P. Pal, "Sparse sensing with co-prime samplers and arrays," *IEEE Transactions on Signal Processing*, vol. 59, no. 2, pp. 573–586, Feb 2011.
- [19] M. Elad, *Sparse and redundant representations: from theory to applications in signal and image processing*. New York: Springer, 2010, oCLC: ocn646114450.
- [20] D. L. Donoho and M. Elad, "Optimally sparse representation in general (nonorthogonal) dictionaries via l_1 minimization," *Proceedings of the National Academy of Sciences*, vol. 100, no. 5, pp. 2197–2202, 2003. [Online]. Available: <http://www.pnas.org/content/100/5/2197>
- [21] R. Gribonval and M. Nielsen, "Sparse representations in unions of bases," *IEEE Transactions on Information Theory*, vol. 49, no. 12, pp. 3320–3325, Dec 2003.
- [22] M. F. Duarte and Y. C. Eldar, "Structured compressed sensing: From theory to applications," *IEEE Transactions on Signal Processing*, vol. 59, no. 9, pp. 4053–4085, Sep. 2011.
- [23] D. L. Donoho, M. Elad, and V. N. Temlyakov, "Stable recovery of sparse overcomplete representations in the presence of noise," *IEEE Transactions on Information Theory*, vol. 52, no. 1, pp. 6–18, Jan 2006.
- [24] S. Jorak, "Sparse recovery and kronecker products," in *2010 44th Annual Conference on Information Sciences and Systems (CISS)*, March 2010, pp. 1–4.
- [25] Y. C. Pati, R. Rezaifar, and P. S. Krishnaprasad, "Orthogonal matching pursuit: recursive function approximation with applications to wavelet decomposition," in *Proceedings of 27th Asilomar Conference on Signals, Systems and Computers*, Nov 1993, pp. 40–44 vol.1.
- [26] J. A. Tropp and A. C. Gilbert, "Signal recovery from random measurements via orthogonal matching pursuit," *IEEE Transactions on Information Theory*, vol. 53, no. 12, pp. 4655–4666, Dec 2007.
- [27] R. Schmidt, "Multiple emitter location and signal parameter estimation," *IEEE Transactions on Antennas and Propagation*, vol. 34, no. 3, pp. 276–280, March 1986.
- [28] J. Li, P. Stoica, and Z. Wang, "On robust capon beamforming and diagonal loading," in *2003 IEEE International Conference on Acoustics, Speech, and Signal Processing, 2003. Proceedings. (ICASSP '03)*, vol. 5, April 2003, pp. V–337.
- [29] S. Boll, "Suppression of acoustic noise in speech using spectral subtraction," *IEEE Transactions on Acoustics, Speech, and Signal Processing*, vol. 27, no. 2, pp. 113–120, April 1979.
- [30] D. Griffin, "Signal estimation from modified short-time Fourier transform," and *Signal Processing IEEE Transactions on Acoustics, Speech, and Signal Processing*, vol. 32, no. 2, pp. 236–243, Apr. 1984.
- [31] J. Allen, "Short term spectral analysis, synthesis, and modification by discrete fourier transform," *IEEE Transactions on Acoustics, Speech, and Signal Processing*, vol. 25, no. 3, pp. 235–238, June 1977.